Geology

Gouge graphitization and dynamic fault weakening during the 2008 Mw 7.9 Wenchuan earthquake

Li-Wei Kuo, Haibing Li, Steven A.F. Smith, Giulio Di Toro, John Suppe, Sheng-Rong Song, Stefan Nielsen, Hwo-Shuenn Sheu and Jialiang Si

Geology 2014;42;47-50
doi: 10.1130/G34862.1

Notes

Gouge graphitization and dynamic fault weakening during the 2008 Mw 7.9 Wenchuan earthquake

Li-Wei Kuo[1,2*], Haibing Li[2], Steven A.F. Smith[3†], Giulio Di Toro[3,4], John Suppe[1], Sheng-Rong Song[1], Stefan Nielsen[3§], Hwo-Shuenn Sheu[5], and Jialiang Si[2]

[1]National Taiwan University, 10617 Taipei, Taiwan
[2]State Key Laboratory of Continental Tectonic and Dynamics, Institute of Geology, Chinese Academy of Geological Sciences, Beijing 100037, China
[3]Instituto Nazionale di Geofisica e Vulcanologia (INGV), 00143 Rome, Italy
[4]Università di Padova, 35122 Padua, Italy
[5]National Synchrotron Radiation Research Center, 30076 Hsinchu, Taiwan

ABSTRACT

The Longmenshan fault that ruptured during the 2008 Mw 7.9 Wenchuan (China) earthquake was drilled to a depth of 1200 m, and fault rocks including those in the 2008 earthquake slip zone were recovered at a depth of 575–595 m. We report laboratory strength measurements and microstructural observations from samples of slip zone fault rocks at deformation conditions expected for coseismic slip at borehole depths. Results indicate that the Longmenshan fault at this locality is extremely weak at seismic slip rates. In situ synchrotron X-ray diffraction analysis indicates that graphite was formed along localized slip zones in the experimental products, similar to the occurrence of graphite in the natural principal slip zone of the 2008 Wenchuan rupture. We surmise that graphitization occurred due to frictional heating of carbonaceous minerals. Because graphitization was associated with strong dynamic weakening in the experiments, we further infer that the Longmenshan fault was extremely weak at borehole depths during the 2008 Wenchuan earthquake, and that enrichment of graphite along localized slip zones could be used as an indicator of transient frictional heating during seismic slip in the upper crust.

INTRODUCTION

The northeast-southwest–trending Longmenshan thrust belt borders the western margin of the Sichuan basin in China (Fig. 1A). On 12 May 2008, the main Longmenshan fault (Beichuan-Yingxiu rupture zone) ruptured in a Mw 7.9 earthquake near Wenchuan in southeast Tibet, producing a 240-km-long surface rupture zone (Xu et al., 2009) (Fig. 1A). The typical surface slip along the rupture trace was 3–4 m, with a maximum slip of ~9.5 m near the town of Hongkou in Wenchuan. The coseismic slip velocity was estimated to be in the range of 1–3 m/s (Xu et al., 2010).

To investigate the processes associated with large earthquakes, the Wenchuan Earthquake Fault Scientific Drilling-1 Project (WFSD-1) was initiated less than one year after the mainshock, with the intention of penetrating the Longmenshan fault at depth (Li et al., 2013). A borehole was drilled to a depth of 1200 m, ~40 km northeast of the epicentral area (Fig. 1A). At 570 m depth, the borehole passed from the Pengguan complex (diorite, porphyrite, volcanic rocks, and pyroclastics) into the Xujiahe Formation (coal-bearing sandstone), broadly marking the location of the Longmenshan fault zone (Fig. 1B). Detailed structural analysis of recovered borehole materials indicated that the Longmenshan fault is a broad zone of damage between 575 and 595 m depth (mainly within the Xujiahe Formation) containing fault breccias, cataclasites, and fault gouges.

At a depth of 590 m, toward the bottom of the fault zone, a 54-cm-thick zone of black fault gouge was recognized, containing highly reflective slip surfaces with slickenlines (Fig. 1C). In one location, the black gouge zone is cut by an ~200-μm-thick ultrafine-grained slip zone (Fig. 1D). Based on microstructural observations, it was suggested that this is the principal slip zone (PSZ) that ruptured in this location during the 2008 Wenchuan earthquake (Li et al., 2013). A distinguishing characteristic of the thin PSZ is the presence of graphite-rich layers (containing >60 wt% graphite) (Fig. 1D) that were not identified in the surrounding black gouge zones or elsewhere in the fault zone (Si et al., 2012).

In this paper, we report mechanical and microstructural data from rotary-shear friction experiments that applied seismic slip pulses on fault gouges of WFSD-1. By in situ synchrotron X-ray diffraction (XRD) analysis, we investigated the processes within gouges deformed under earthquake-like conditions.

EXPERIMENTAL METHODS

Rotary-shear friction experiments were performed on the black gouges retrieved from the WFSD-1 borehole cores with the aim of reproducing the estimated coseismic slip conditions at borehole depths of 590 m (i.e., the depth of the PSZ in the borehole). Seven experiments were performed at room temperature and room humidity using the slow- to high-velocity rotary-shear friction apparatus (SHIVA) at the high-pressure–high-temperature laboratories of the Istituto Nazionale di Geofisica e Vulcanologia (INGV, Rome, Italy) (Di Toro et al., 2010). The black gouges were first gently crushed and sieved to a grain size of <250 μm. In each experiment, 5 g of gouge, corresponding to an initial layer thickness of ~3 mm, was poured into a ring-shaped (55 mm external, 35 mm internal diameter) sample holder for noncohesive materials (Smith et al., 2013). Maximum slip rates during the experiments were 3.0–3.2 m/s, normal stresses were held constant at 5–25 MPa, the acceleration and deceleration rates were 6 m/s^2, and total displacements were as much as 3.0 m (see Item DR1 in the GSA Data Repository[1]). No gouge extrusion was observed during the experiments.

After the experiments, microstructural observations of the deformed gouge layers were conducted on petrographic sections cut approximately parallel to the slip direction and perpendicular to the gouge layers using a FEI QUANTA 200F field-emission scanning electron microscope equipped with energy dispersive spectrometer at the National Taiwan University. The mineralogy of the gouge layers was determined with high spatial resolution using in situ X-ray diffraction analysis at the BL01C2 beamline of the National Synchrotron Radiation Research Center in Taiwan (see Item DR2) (Wang et al., 2011).

RESULTS

Mechanical results of four experiments at different normal stresses are shown in Figure 2A. The most significant mechanical response of the

*E-mail: liweikuo@ntu.edu.tw.
†Current address: Department of Geology, University of Otago, Dunedin 9054, New Zealand.
§Current address: Rock Mechanics Laboratory, Earth Sciences Department, University of Durham, South Road, Durham DH13LE, UK.

[1]GSA Data Repository item 2014012, Item DR1 (summary of experimental conditions), Item DR2 (description of sample preparation and method of in-situ synchrotron X-ray analysis), Item DR3 (description of starting material compacted to 12 MPa), and Item DR4 (computation of temperature evolution along the principal slip zone formed at 15 MPa), is available online at www.geosociety.org/pubs/ft2014.htm, or on request from editing@geosociety.org or Documents Secretary, GSA, P.O. Box 9140, Boulder, CO 80301, USA.

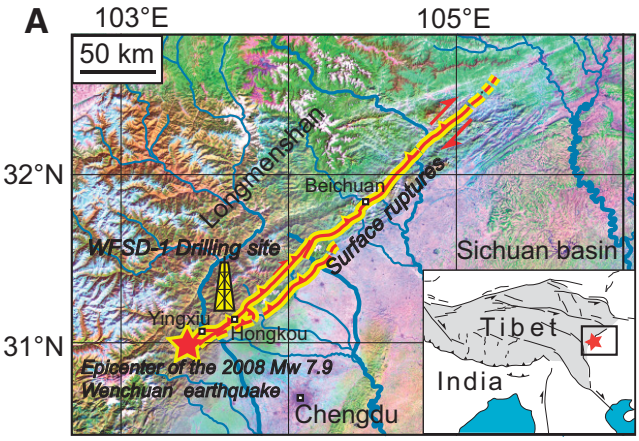

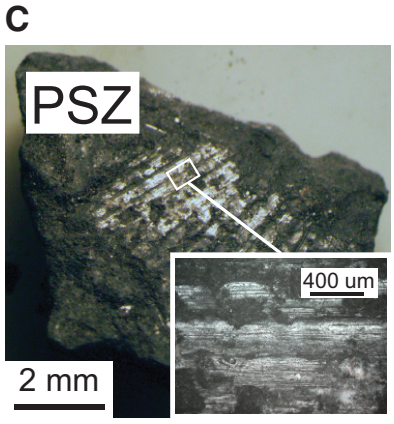

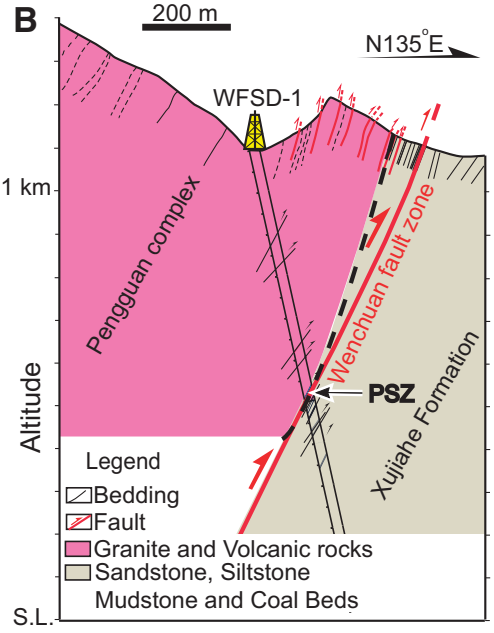

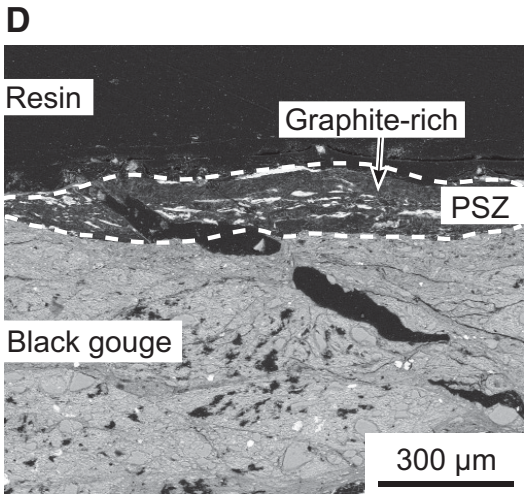

Figure 1. Geological setting of the 2008 Mw 7.9 Wenchuan (China) earthquake and location of the Wenchuan Earthquake Fault Scientific Drilling-1 Project (WFSD-1) drilling site. A: Location of WFSD-1 drilling site and the 240-km-long surface ruptures associated with the Mw 7.9 earthquake along the margin of the Longmenshan mountains and Sichuan Basin. Red star marks epicenter of the mainshock. Inset is a schematic drawing of the Tibetan Plateau. B: Cross section of the WFSD-1 drilling site showing the Longmenshan fault zone and surrounding formations encountered in the borehole (after Li et al., 2012). Bold red line is the principal slip zone (PSZ) activated during the 2008 mainshock rupture, identified in the borehole at 589.2 m depth. Dashed black line is the boundary of lithological formations. C: Photograph of highly reflective surface with slickenlines recognized within the black gouges. D: Backscattered scanning electron microscope image of a thin section cut through part of the PSZ (within white dashed lines). Thickness of the PSZ in this location is ~200 μm and the PSZ is characterized by a local enrichment of graphite-rich layers.

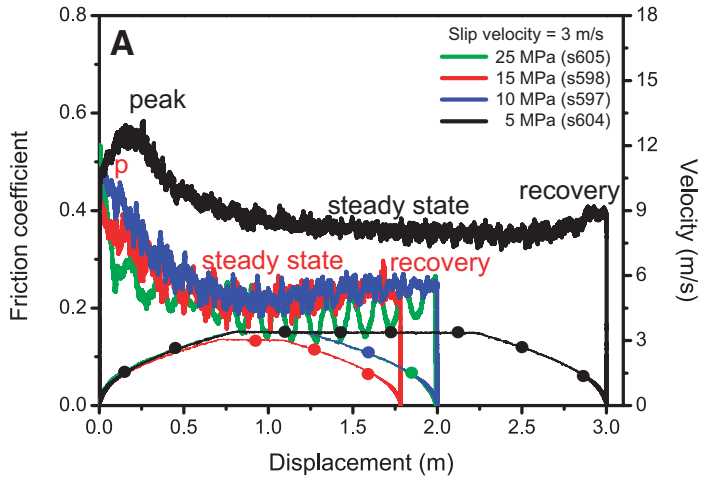

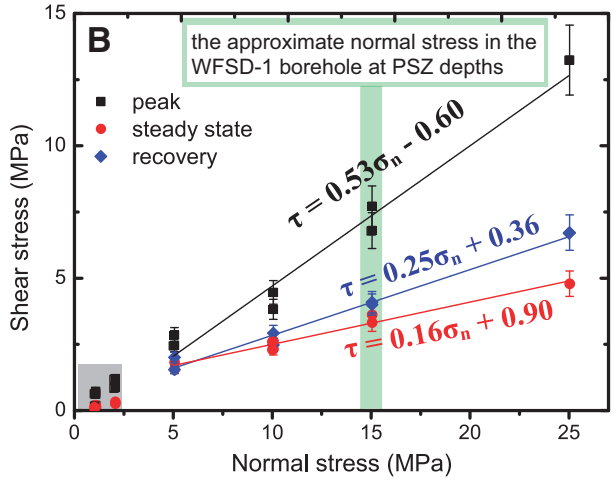

Figure 2. Frictional strength at high velocity of black gouges from the Longmenshan slip zone (China). A: Friction coefficient (shear stress / normal stress) versus displacement for four experiments (s597, s598, s604, and s605) carried out at different normal stresses. Circles indicate slip velocity curves. B: Shear stress versus normal stress at peak, steady state, and recovery for all experiments at 3 m/s slip velocity. Green vertical bar represents the approximate normal stress in the Wenchuan Earthquake Fault Scientific Drilling-1 Project (WFSD-1) borehole at principal slip zone (PSZ) depths (589.2 m). Gray box displays normal and shear stress ranges covered by a majority of previous experiments on fault gouges up to 3 m/s slip velocity. Data points within the gray box are experiments on carbonaceous materials and graphite performed at 1–2 MPa normal stress and up to 1.3 m/s slip velocity by Oohashi et al. (2011).

gouge layers during high-velocity shearing is a decrease (abrupt in the case of normal stress >5 MPa) in the friction coefficient (shear stress/normal stress) from a peak of ~0.5 to a steady-state between 0.4 at 5 MPa normal stress and 0.15–0.18 at 10–25 MPa normal stress. These mechanical data are consistent with previous experiments performed on carbonaceous materials at lower normal stresses and slip rates (gray box in Fig. 2B) (Oohashi et al., 2011). A slight strength recovery (corresponding to an increase in the friction coefficient of ~0.02) was observed during the final deceleration at the end of slip (Fig. 2A). At seismic slip rates of 3 m/s and normal stresses up to 25 MPa, the peak, steady-state, and final shear stresses increase linearly with normal stress (Fig. 2B). The relatively high steady-state friction coefficient of 0.4 measured at 3.2 m/s and 5 MPa normal stress (Fig. 2A) suggests that the processes triggered in the experiments performed at low normal stresses (≤5 MPa) are different from those at higher normal stresses, at least for displacements of a few meters achieved during coseismic slip events.

Strain localization in the gouge layers during high-velocity slip resulted in the development of an experimental PSZ cut by a smooth and light reflective surface, similar to those identified in the black gouges in the WFSD-1 borehole (cf. Figs. 3A and 1C). Compared to the starting material (<250 µm in size; see Item DR3) the experimental PSZs show a marked reduction in grain size (<10 µm, FE-SEM observations) within a layer 30–80 µm thick (Fig. 3B).

The black gouges used as starting materials are composed of quartz (~50 wt%), carbonaceous materials (mainly poorly crystalline anthracite; see Item DR3) (~25 wt%), clay minerals (~20 wt%: illite, chlorite, and kaolinite), and minor calcite (<5 wt%) (Fig. 4). In situ synchrotron mineralogical characterization indicates that at low normal stresses (5 MPa), the composition of the experimental PSZ is unchanged with respect to the starting material (Fig. 4). However, at normal stresses >10 MPa, the PSZ is significantly enriched in graphite (see the growth of graphite [101] broadband peak in Fig. 4) and depleted in calcite, illite, and chlorite with respect to the starting material.

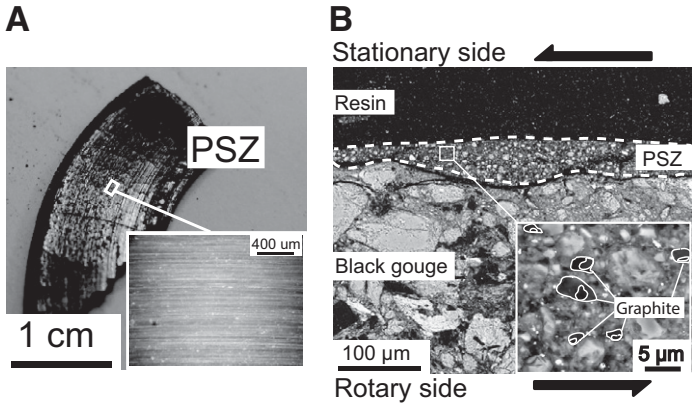

Figure 3. Microstructural characteristics of experimentally deformed black gouges. A: Photograph of highly reflective surface of the principal slip zone (PSZ) lined by slickenlines and grooves that track the rotary motion of the gouge holder (experiment s598, 15 MPa). B: Backscattered scanning electron microscope (SEM) image of thin section cut approximately parallel to the slip direction and perpendicular to the deformed gouge layer (experiment s598, 15 MPa). White dashed lines enclose localized and fine-grained PSZ between 25 and 125 µm thick that developed adjacent to the stationary side of the gouge holder. Inset backscattered SEM image shows detail of small graphite particles that we suggest formed by heating of carbonaceous materials (mainly anthracite) within the PSZ during experiments at >10 MPa normal stress.

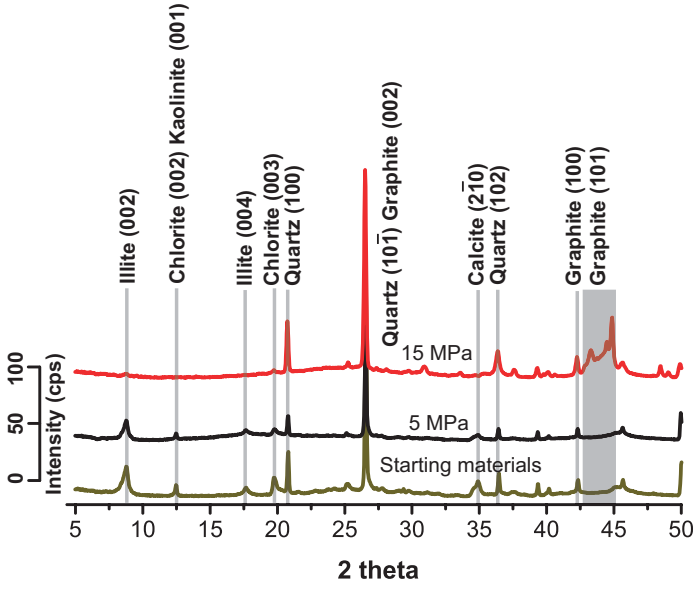

Figure 4. Mineralogical changes within the experimental principal slip zones (PSZs) determined by in situ synchrotron X-ray analyses (see Item DR2 [see footnote 1]). The undeformed starting material and the PSZ formed at 5 MPa are rich in quartz, with calcite, chlorite, illite, and minor graphite as the other phases. At >10 MPa, the PSZs are characterized by the absence of calcite, illite, and chlorite, but a strong enrichment in graphite. cps—counts per second.

DISCUSSION AND CONCLUSION

In the present study, graphite was produced during shearing of carbonaceous gouge at conditions approaching those estimated for the 2008 Wenchuan earthquake rupture at borehole depths: slip rates up to 3 m/s, slip distances of a few meters, and normal stress up to 25 MPa. Graphite was not detected in the sheared gouge of experiments performed at 5 MPa normal stress, and the friction coefficient in those experiments remained relatively high (steady-state of 0.4). Experiments performed at the normal stresses closer to those expected at WFSD-1 borehole depths (~15 MPa) revealed drastic dynamic weakening (Figs. 2 and 3) and graphitization of the sheared gouge (Fig. 4).

Combining the microstructural and mineralogical observations, we propose that at normal stresses >10 MPa, the frictional power density (Di Toro et al., 2011), which is the product of shear stress and slip velocity, was sufficiently high (>10 MW m^{-2} for experiments performed at normal stress >10 MPa) within the localized PSZs to trigger mechanically and thermally induced transformation of the carbonaceous components within the black gouges: this resulted in the formation of graphite in sufficient amounts to be detected by synchrotron XRD analysis (Fig. 4). The temperature evolution in the experiment at 15 MPa was computed using the experimentally measured frictional power and taking into consideration the estimated heat sinks due to dehydration reactions, following the studies of Sulem and Famin (2009) and Brantut et al. (2011) (see Item DR4). According to this estimate, a maximum temperature of ~1200 °C was ~0.10 s after slip deceleration started (~1.6 m of slip). During frictional sliding at seismic slip rates, reactions can occur at lower bulk temperatures than in static heating experiments (Di Toro et al., 2011), mainly because (1) shear induces plastic deformation and fracturing of grains and exposes new and highly reactive and catalytic surfaces (which lowers the activation energy of the reaction), and (2) flash heating (Rice, 2006) at the asperity scale results in abrupt local increases in temperature (which triggers the reactions). Consistent with this and similar interpretations, Bustin et al. (1995) directly measured temperature of graphitization on anthracite of ~900 °C. This temperature estimate is consistent with (1) the breakdown in the sheared gouges (Fig. 4) of illite (T_{break} ~900 °C) and calcite (T_{break} ~800 °C), and (2) the frictional power dissipated in our experiments

(10.8 MW m^{-2}), which results in an estimated temperature increase (upper bound) of 1200 °C (see Item DR4).

Graphitization (crystallization) of carbonaceous materials exposed to frictional heating was previously recognized to take place under anoxic conditions (Oohashi et al., 2011), which can be expected to occur at depth within the Longmenshan fault zone during seismic faulting. In the experiments, the ambient conditions were initially not anoxic, but we speculate that air cannot be introduced into the slip zone during shearing because of (1) the application of normal load and centrifugal forces, and (2) gas escape from the slip zone due to the breakdown of calcite, illite, chlorite, and carbonaceous materials. Thus, the transformation of carbonaceous materials into graphite could have been facilitated during slip by (1) the generation of CO_2 from the combustion of preexisting O_2 in pores, with graphite being produced at the initiation of sliding (graphite generation after this initial stage will occur in an anoxic environment); and (2) the release of CO_2 due to thermal decomposition of calcite and oxidation of graphite (Han et al., 2007), which reduces the partial pressure of O_2.

The short weakening distance (<0.5 m; Fig. 2A) in our experiments suggests that the cumulative frictional heat generated during coseismic slip of several meters would be small (see Item DR1), and thus the coseismic thermal perturbation within the fault zone is expected to be small (see Item DR4). This finding is in agreement with preliminary temperature measurements performed less than one year after drilling, which detected a small thermal anomaly (<0.15 °C) (Brodsky et al., 2012) around the PSZ, indicating a very low (~0.1) dynamic friction coefficient during the Wenchuan earthquake (Brodsky et al., 2012).

The localized formation of graphite in the PSZ of both the Longmenshan fault (Fig. 1D) and in our experiments (Fig. 3B) is in contrast to the absence of graphite in, respectively, nearby fault rocks and the experimental starting material. We conclude that (1) our experiments reproduced some of the deformation conditions experienced at borehole depths during the 2008 Wenchuan earthquake; (2) graphitization of principal slip zone gouges took place during the 2008 earthquake, and probably previous earthquakes; and (3) the experimental data measured at normal stresses of 10–25 MPa indicate dynamic weakening of the Longmenshan fault at shallow crustal depths.

We envision that gouge graphitization may be a widespread process along the Longmenshan fault (Li et al., 2012; Togo et al., 2011) and other carbonaceous-rich fault zones (e.g., Oohashi et al., 2011, 2012). Because graphite is a relatively stable mineral (Beyssac et al., 2002), the localized enrichment of graphite in thin slip zones could indicate transient frictional heating during ancient seismic events.

ACKNOWLEDGMENTS

This research used materials provided by the "Wenchuan Earthquake Fault Scientific Drilling" of the National Science and Technology Planning Project (China). We thank all drilling operation staff of the Wenchuan Earthquake Fault Scientific Drilling Center. Part of this work was supported by a European Research Council Starting Grant (205175) to Di Toro, the "Wenchuan Earthquake Fault Scientific Drilling" of the National Science and Technology Planning Project and the National Natural Science Foundation of China (41330211) to Li, and Taiwan (Republic of China) National Science Council and National Taiwan University grants to Suppe and Song. We thank three anonymous reviewers for their positive and constructive comments, and editor Bob Holdsworth for his help throughout the publication process.

REFERENCES CITED

Beyssac, O., Goffe, B., Chopin, C., and Rouzaud, J.N., 2002, Raman spectra of carbonaceous material in metasediments: A new geothermometer: Journal of Metamorphic Geology, v. 20, p. 859–871, doi:10.1046/j.1525-1314.2002.00408.x.

Brantut, B., Sulem, J., and Schubnel, A., 2011, Effect of dehydration reactions on earthquake nucleation: Stable sliding, slow transients, and unstable slip: Journal of Geophysical Research, v. 116, B05304, doi:10.1029/2010JB007876.

Brodsky, E.E., Li, H., Mori, J.J., Kano, Y., and Xue, L., 2012, Frictional stress measured through temperature profiles in the Wenchuan Scientific Fault Zone Drilling project: Eos (Transactions, American Geophysical Union), v. 93, fall meeting supplement, abs. T44B–07.

Bustin, R.M., Ross, J.V., and Rouzaud, J.-N., 1995, Mechanisms of graphite formation from kerogen: Experimental evidence: International Journal of Coal Geology, v. 28, p. 1–36, doi:10.1016/0166-5162(95)00002-U.

Di Toro, G., and 12 others, 2010, From field geology to earthquake simulation: A new state-of-the-art tool to investigate rock friction during the seismic cycle (SHIVA): Rendiconti Lincei-Scienze Fisiche e Naturali, v. 21, p. 95–114, doi:10.1007/s12210-010-0097-x.

Di Toro, G., Han, R., Hirose, T., De Paola, N., Nielsen, S., Mizoguchi, K., Ferri, F., Cocco, M., and Shimamoto, T., 2011, Fault lubrication during earthquakes: Nature, v. 471, p. 494–498, doi:10.1038/nature09838.

Han, R., Shimamoto, T., Hirose, T., Ree, J.-H., and Ando, J., 2007, Ultralow friction of carbonate faults caused by thermal decomposition: Science, v. 316, p. 878–881, doi:10.1126/science.1139763.

Li, H., Xu, Z., Si, J., Song, S.R., Sun, Z., and Chevalier, M.-L., 2012, Wenchuan earthquake fault Scientific Drilling Program (WFSD): Overview and results: Eos (Transactions, American Geophysical Union), v. 93, fall meeting supplement, abs. T44B–01.

Li, H., and 11 others, 2013, Characteristics of the fault-related rocks, fault zones and the principal slip zone in the Wenchuan earthquake Fault Scientific Drilling Hole-1 (WFSD-1): Tectonophysics, v. 584, p. 23–42, doi:10.1016/j.tecto.2012.08.021.

Oohashi, K., Hirose, T., and Shimamoto, T., 2011, Shear-induced graphitization of carbonaceous materials during seismic fault motion: experiments and possible implications fault mechanics: Journal of Structural Geology, v. 33, p. 1122–1134, doi:10.1016/j.jsg.2011.01.007.

Oohashi, K., Hirose, T., Kobayashi, K., and Shimamoto, T., 2012, The occurrence of graphite-bearing fault rocks in the Atotsugawa fault system, Japan: Origins and implications for fault creep: Journal of Structural Geology, v. 38, p. 39–50, doi:10.1016/j.jsg.2011.10.011.

Rice, J. R., 2006, Heating and weakening of faults during earthquake slip: Journal of Geophysical Research, v. 111, B05311, doi:05310.01029/02005JB004006.

Si, J., Li, H., Song, S.R., Kuo, L.W., Pei, J., Chen, P., Hsiao, H., and Wang, H., 2012, Minerals anomalies and their significances in fault rocks along the front Longmenshan fault: Eos (Transactions, American Geophysical Union), v. 93, fall meeting supplement, abs. T41D–2628.

Smith, S.A.F., Di Toro, G., Kim, S., Ree, J.-H., Nielsen, S., Billi, A., and Spiess, R., 2013, Coseismic recrystallization during shallow earthquake slip: Geology, v. 41, p. 63–66, doi:10.1130/G33588.1.

Sulem, J., and Famin, V., 2009, Thermal decomposition of carbonates in fault zones: Slip-weakening and temperature-limiting effects: Journal of Geophysical Research, v. 114, p. B03309, doi:10.1029/2008JB006004.

Togo, T., Shimamoto, T., Ma, S., Wen, X., and He, H., 2011, Internal structure of Longmenshan fault zone at Hongkou outcrop, Sichuan, China, that caused the 2008 Wenchuan earthquake: Earth Science, v. 24, p. 249–265, doi:10.1007/s11589-011-0789-z.

Wang, C.-C., Yang, C.-C., Yeh, C.-T., Cheng, K.-Y., Chang, P.-C., Ho, M.-L., Lee, G.-H., Shih, W.-J., and Sheu, H.-S., 2011, Reversible solid-state structural transformation of a 1D–2D coordination polymer by thermal de/rehydration processes: Inorganic Chemistry, v. 50, p. 597–603, doi:10.1021/ic1018345.

Xu, C., Liu, Y., Wen, Y., and Wang, R., 2010, Coseismic slip distribution of the 2008 Mw 7.9 Wenchuan earthquake from joint inversion of GPS and InSAR data: Seismological Society of America Bulletin, v. 100, p. 2736–2749, doi:10.1785/0120090253.

Xu, X., Wen, X., Yu, G., Chen, G., Klinger, Y., Hubbard, J., and Shaw, J., 2009, Coseismic reverse- and oblique-slip surface faulting generated by the 2008 Mw7.9 Wenchuan earthquake, China: Geology, v. 37, p. 515–518, doi:10.1130/G25462A.1.

Manuscript received 20 June 2013
Revised manuscript received 22 September 2013
Manuscript accepted 7 October 2013

Printed in USA